Electronic Supplementary Material (ESI) for New Journal of Chemistry.

Supporting Information

One new azido bridged dinuclear copper(II) thiosemicarbazide complex: Synthesis, DNA/protein binding, molecular docking study and cytotoxicity activity

Niladri Biswas[1], Sumit Khanra[2], Arnab Sarkar[3], Shamee Bhattacharjee[3], Deba Prasad Mandal[3], Ankur Chaudhuri[4], Sibani Chakraborty[4], Chirantan Roy Choudhury[1*]

[1]*Department of Chemistry, West Bengal State University, Barasat, Kolkata-700126, India.*

[2]*Department of Chemistry, Indian Institute of Science Education and Research, Kolkata Mohanpur - 741 246, West Bengal, India*

[3]*Department of Zoology, West Bengal State University, Barasat, Kolkata-700126, India.*

[4]*Department of Microbiology, West Bengal State University, Barasat, Kolkata-700126, India.*

* Corresponding author:

Tel: + 91-9836306502

Fax: +91-33-2524-1577

Email: crchoudhury2000@yahoo.com

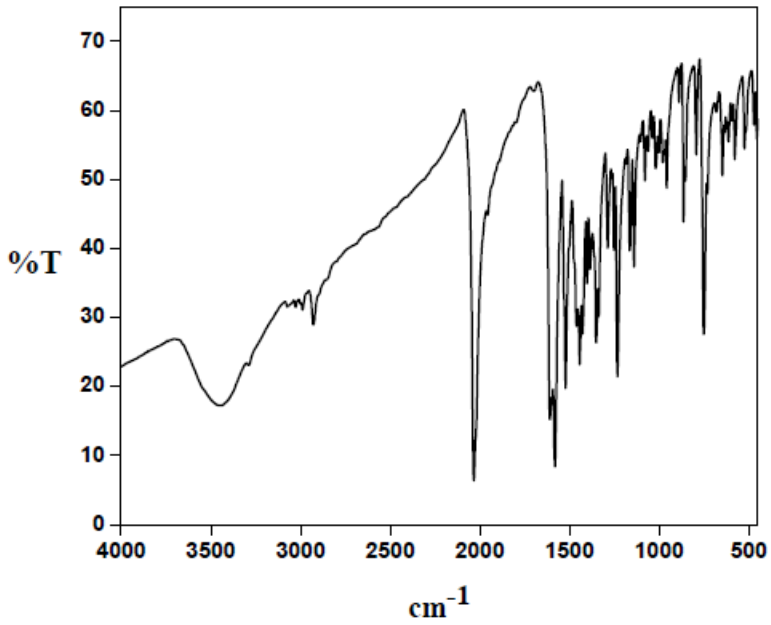

Fig. S1 FT-IR spectra of the copper complex.

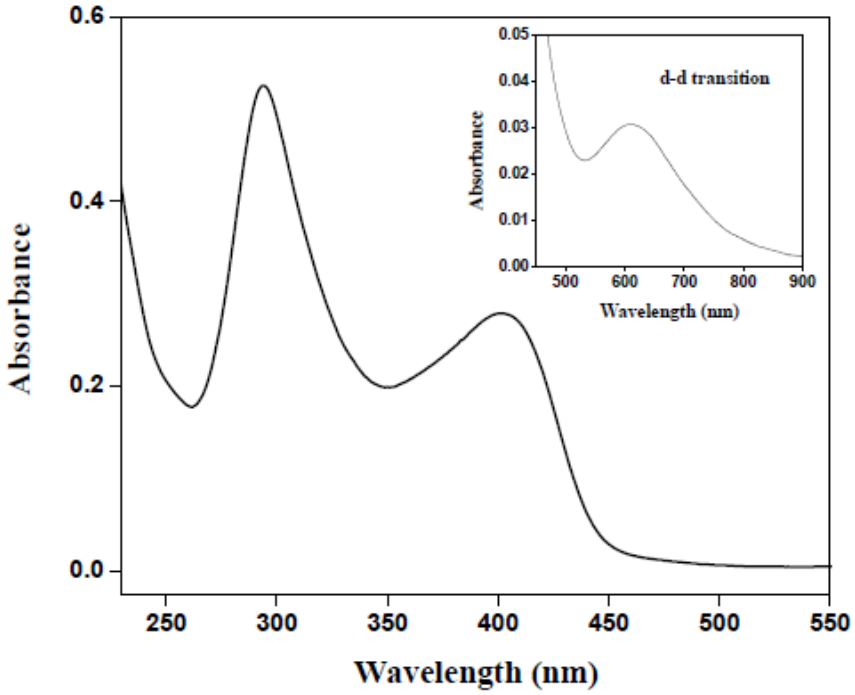

Fig. S 2 Electronic spectra of the copper complex (50 X 10^{-6} M) in Tris-buffer medium. The inset shows d-d transition bands.

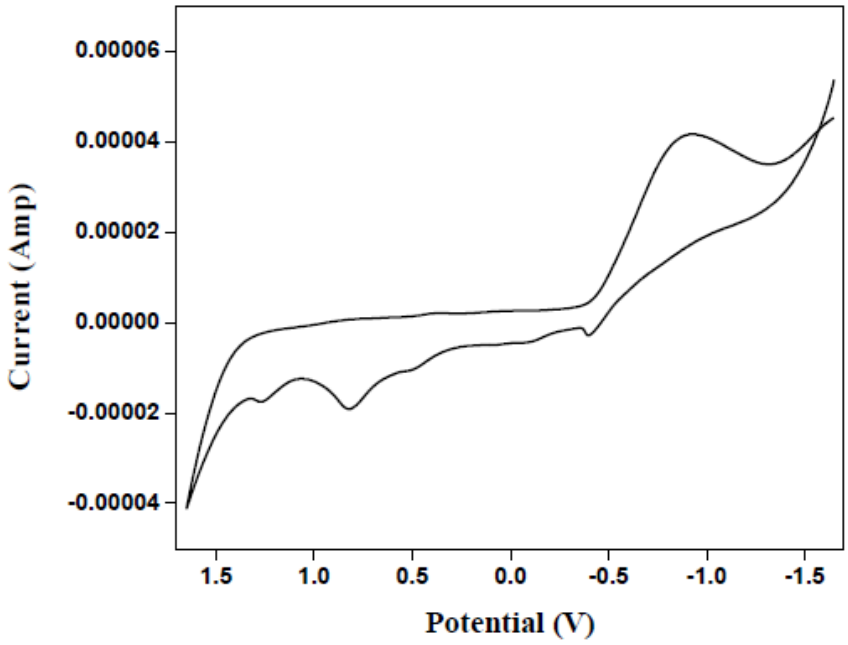

Fig. S 3 Cyclic voltammogram of 10^{-3}M copper complex in Tris-HCl buffer containing 0.1 M TBAP.

Stability of complex 1 in solution

All the biological tests of the complex **1** were performed in Tris- buffer aqueous medium. So the stability of complex **1** in aqueous buffer played an important role in its structure-function relation. To ascertain the integrity of the complex **1**, the following experiments were carried out. An IR spectrum of the residue of **1** obtained after evaporating the aqueous buffer medium was matched with that of a freshly prepared sample of the same. The two spectra matched nicely. The most important evidence of the integrity of the dinuclear structure was obtained by ESI mass spectra in positive mode in aqueous medium. It was recorded in a Agilent 6520 Q-Tof Spectrometer at room temperature in the m/Z range of 0-1000. The molecular ion peak appeared at m/Z 598.9, which could be attributed to the molecular ion $[Cu(L_1)_2(N_3)_2]$ [Fig. S13]. This proved that **1** did not undergo any kind of dissociation in aqueous medium under ordinary condition.

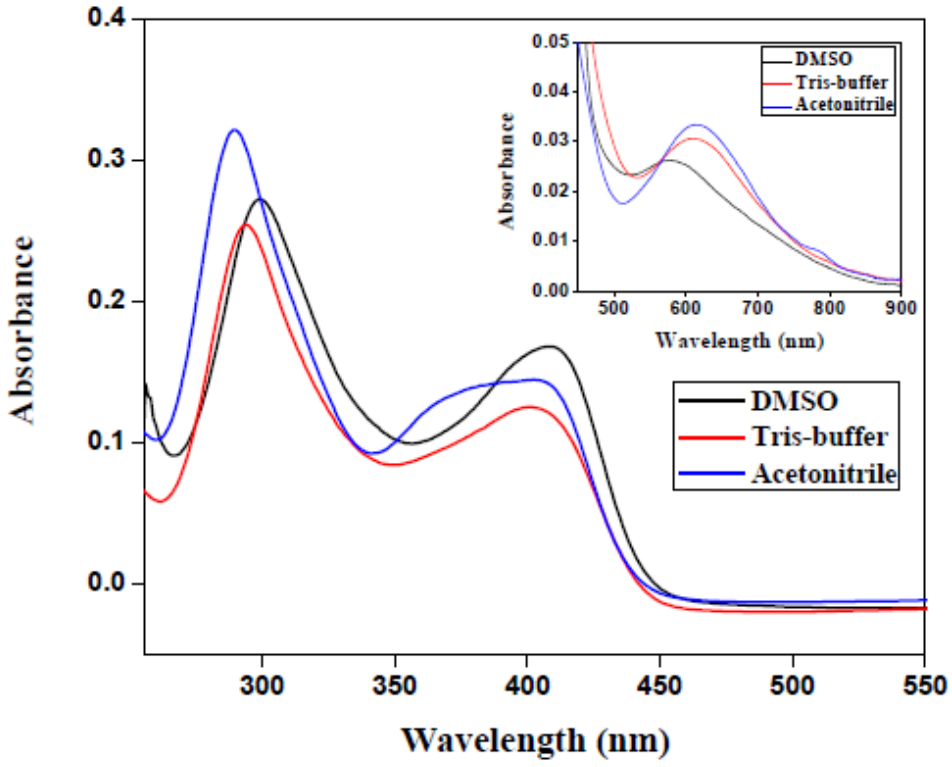

Fig. S 4 UV-Vis spectra of complex **1** in DMSO, Tris-buffer and acetonitrile medium.

Solvents/ medium used	**DMSO**	**Tris-buffer**	**Acetonitrile**
UV-Vis bands	577 (d-d)	609 (d-d)	615 (d-d)
	408 (CT)	401 (CT)	401 (CT)
	299 (CT)	294 (CT)	289 (CT)

T1 UV-Vis band positions of **1** in DMSO, Tris-buffer and acetonitrile medium.

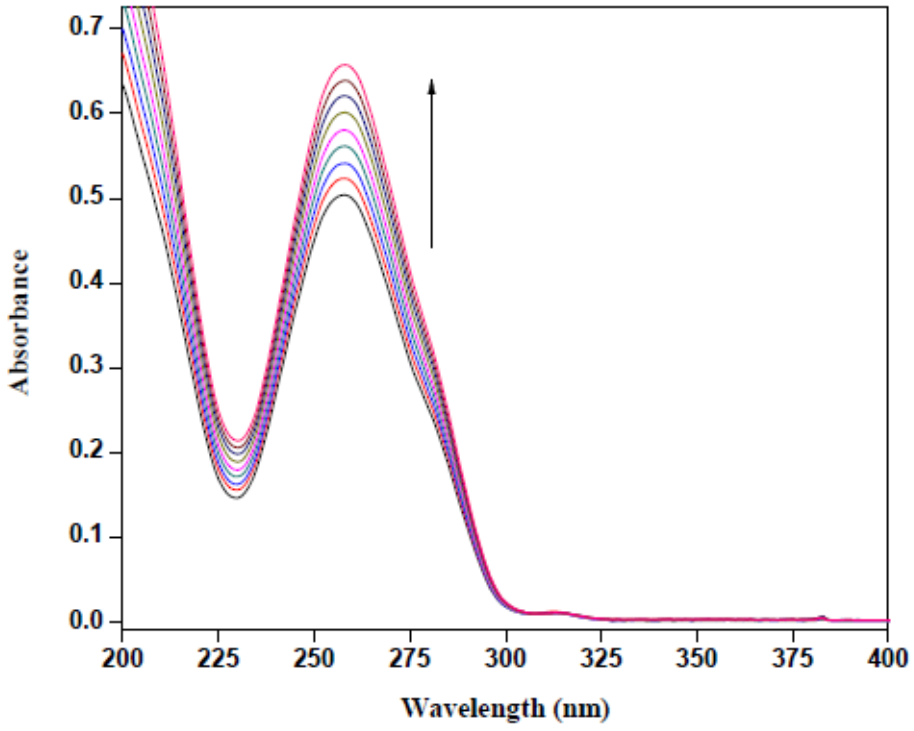

Fig. S5: Absorption spectra in Tris-HCl buffer with gradual addition of CT-DNA in absence of complex 1.[DNA] = 0-110 μM . The arrow shows the absorbance changes on 257 nm with increasing CT-DNA concentration.

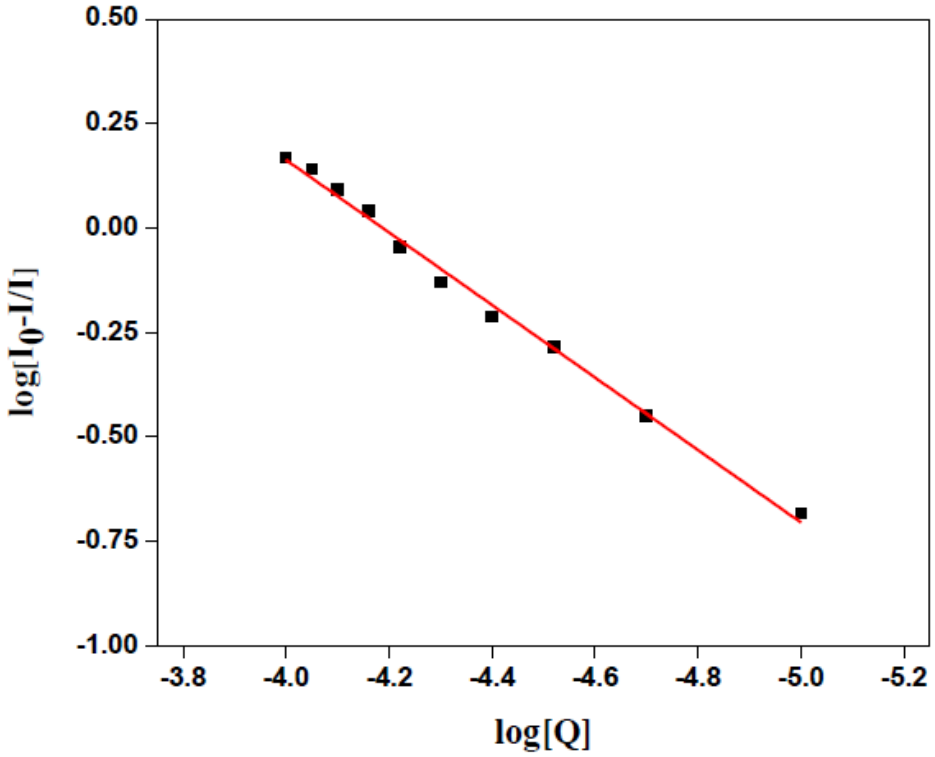

Fig.S 6: Plot of log $[(I_0\text{-}I)/I]$ *vs* log[Q]

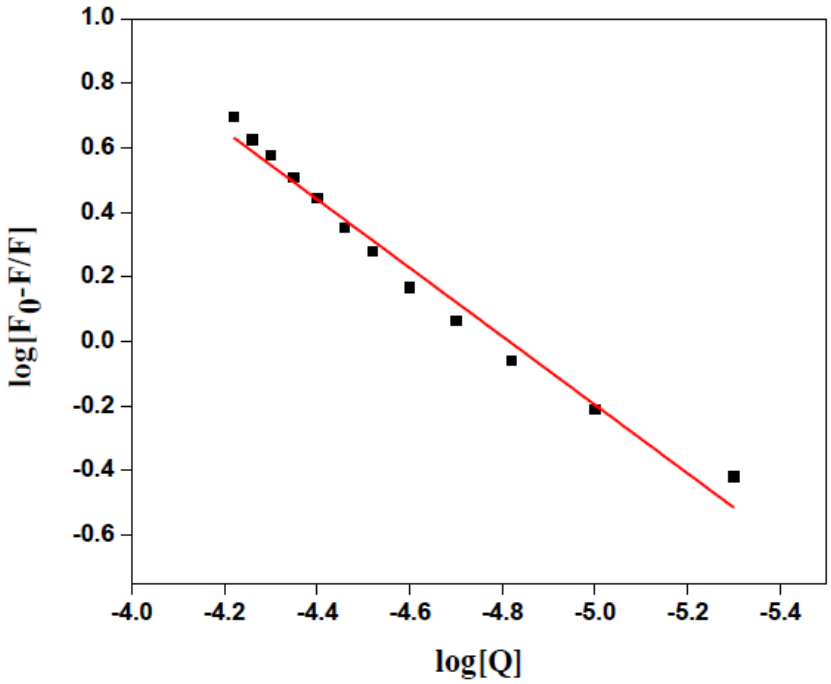

Fig. S 7A: Scatchard plot of the fluorescence titrations of the complex **1** with BSA.

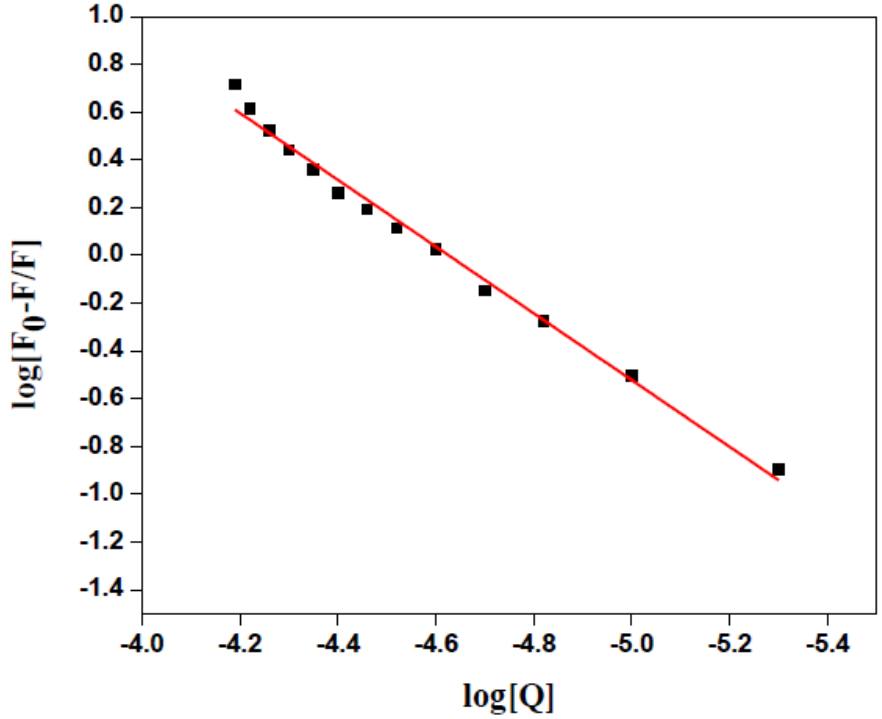

Fig. S 7B: Scatchard plot of the fluorescence titrations of the complex **1** with HSA.

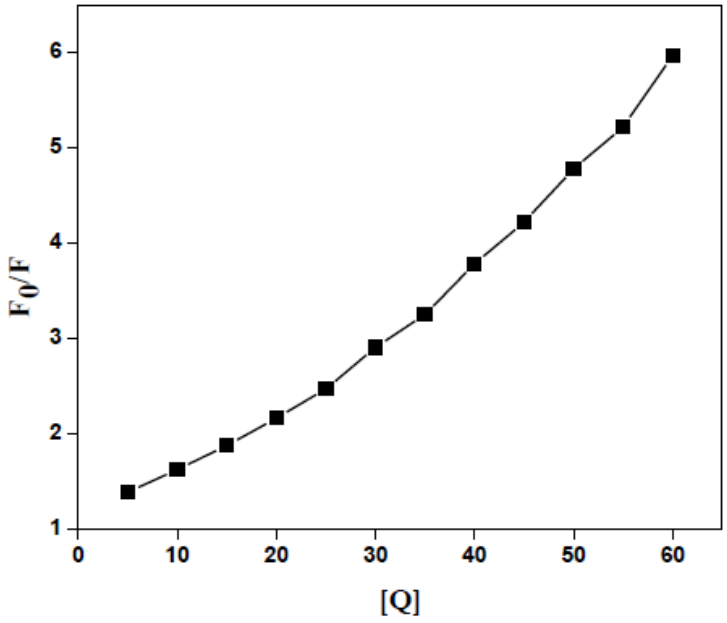

Fig. S 8A : Stern-Volmer non-linear plots of the fluorescence titration of the complex **1** with BSA.

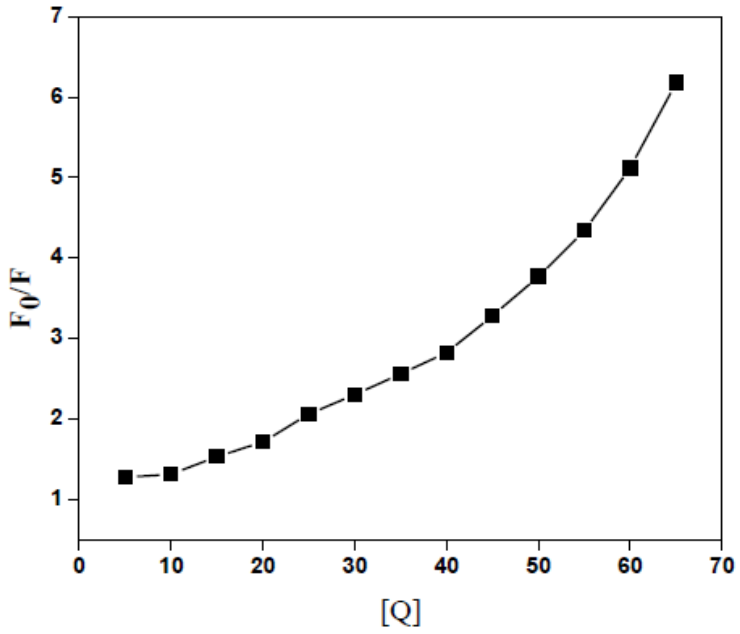

Fig. S 8B: Stern-Volmer non-linear plots of the fluorescence titration of the complex **1** with HSA.

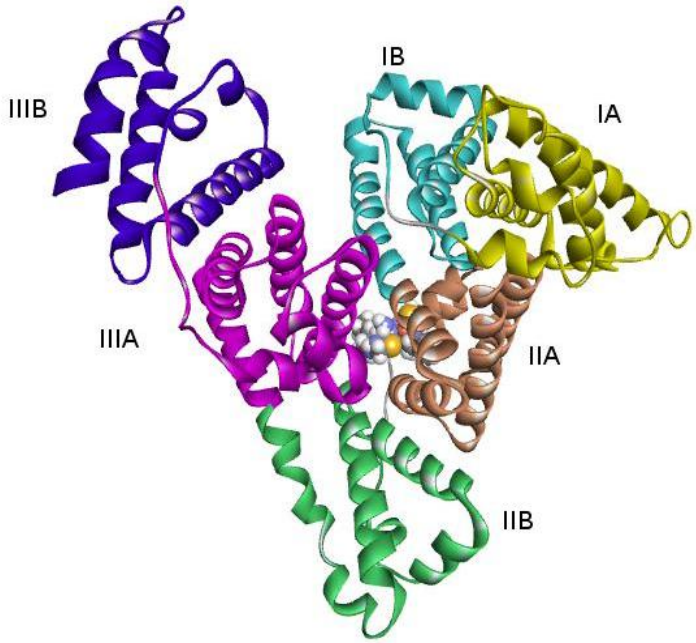

(9A)

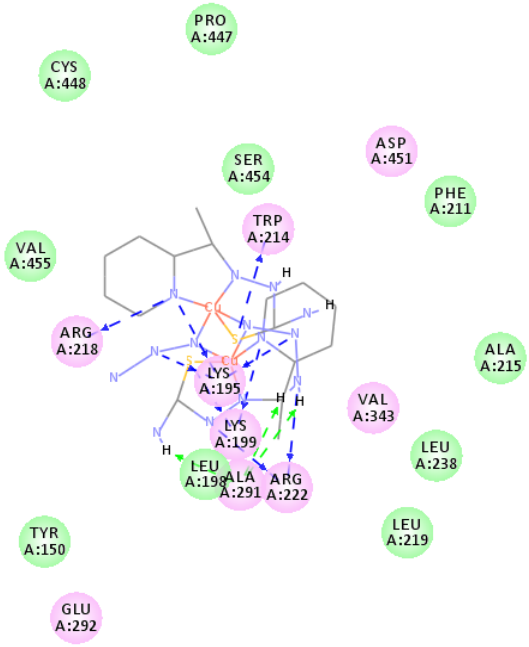

(9B)

Fig. S 9: Docking of complex **1** in the binding site of HSA (PDB ID: 4IW2). (A) The full view of complex **1** in HSA. Representation of complex **1** in CPK mode. (B) 2D representation of intermolecular interaction of HSA with complex **1**. Residues involved in electrostatic and van der Waal's interactions are represented by pink and green circles

respectively. Green and blue dashed lines show main chain and side chain hydrogen bond interactions respectively between HSA and complex **1**.

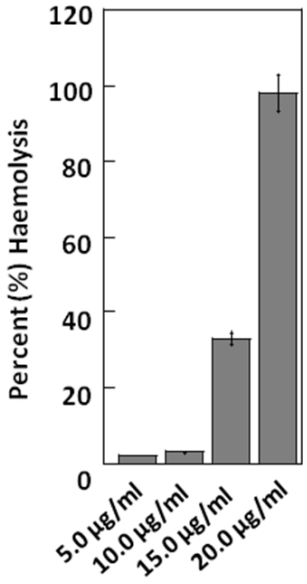

Fig. S 10 Percentage hemolytic activity of on human red blood cells.

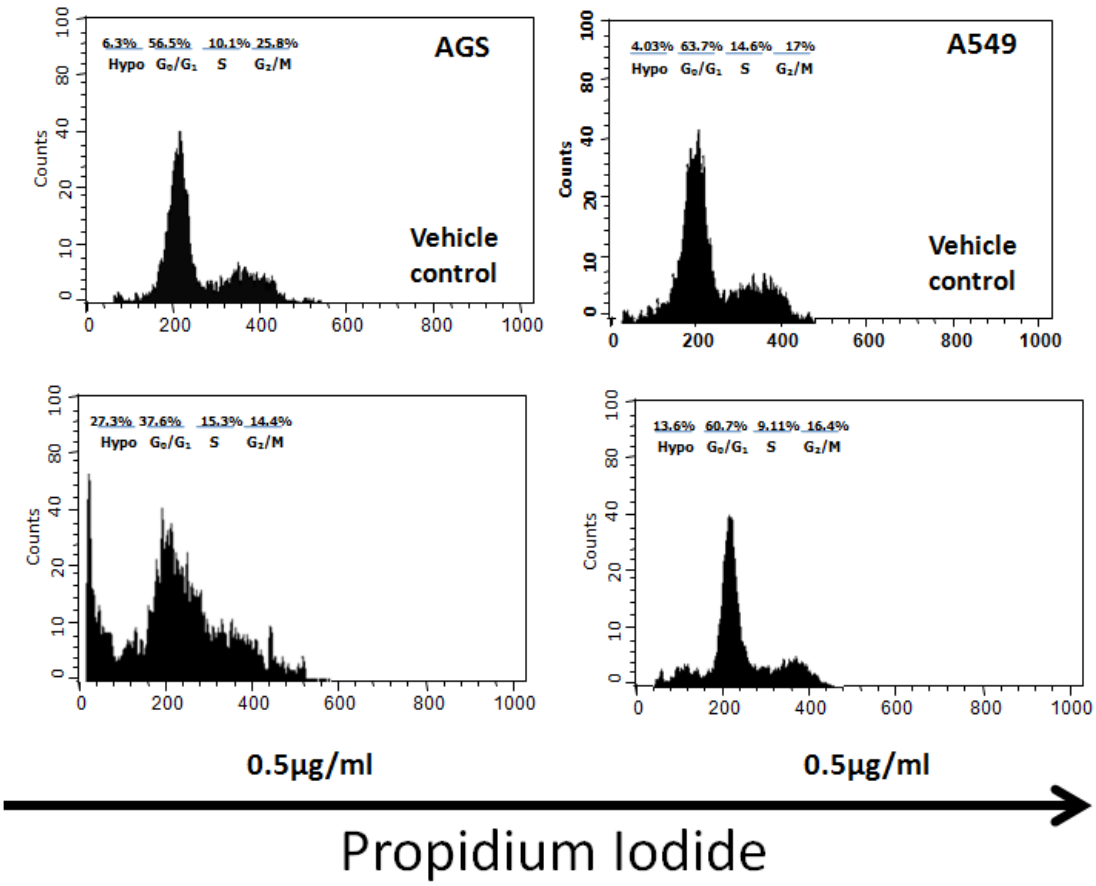

Fig. S 11 Cell cycle analysis of treated and untreated AGS and A549 cells by Flowcytometer using propidium iodide (PI) as DNA-binding fluorochrome.Histogram display of DNA content (x-axis, PI-fluorescence) versus counts (y-axis) has been shown. The upper and lower panels display cell cycle phase distribution of treated and untreated AGS cells with wild type p53 and silenced p53 respectively.

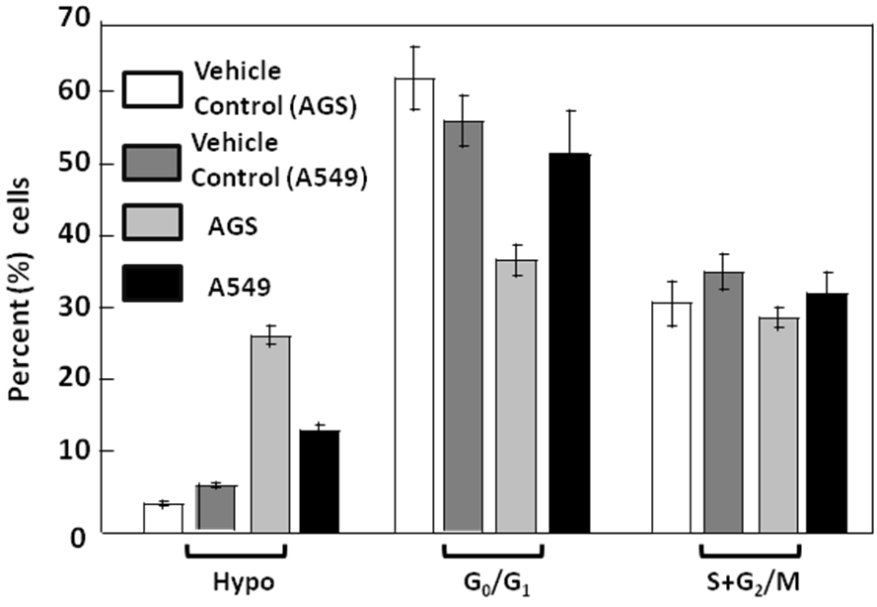

Fig. S 12 Bar diagram representation of cell cycle phase distribution of AGS (with wild type and p53 knock out cells) from different experimental groups.

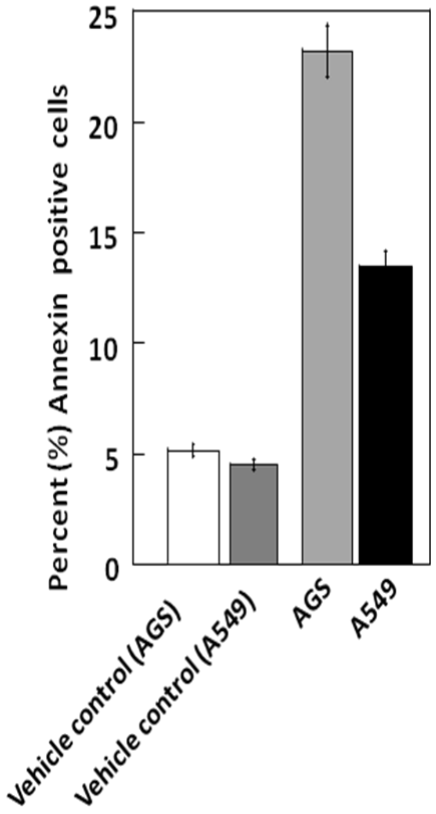

Fig. S 13 Bar diagram representation of percent Annexin V positive AGS cells from different experimental groups are also given in the Fig. **13A** and **13B**. Western Blot detection of proliferative marker, PCNA. Equal loading of protein in the lanes was confirmed by GAPDH. Indicated proteins are represented as bar diagrams of mean + SD of their relative densities as measured from three independent experiments. Each test was performed 3 times and images presented were typical of 3 independent experiments.The data represented as mean+S.D. for the three different experiments performed in triplicate.

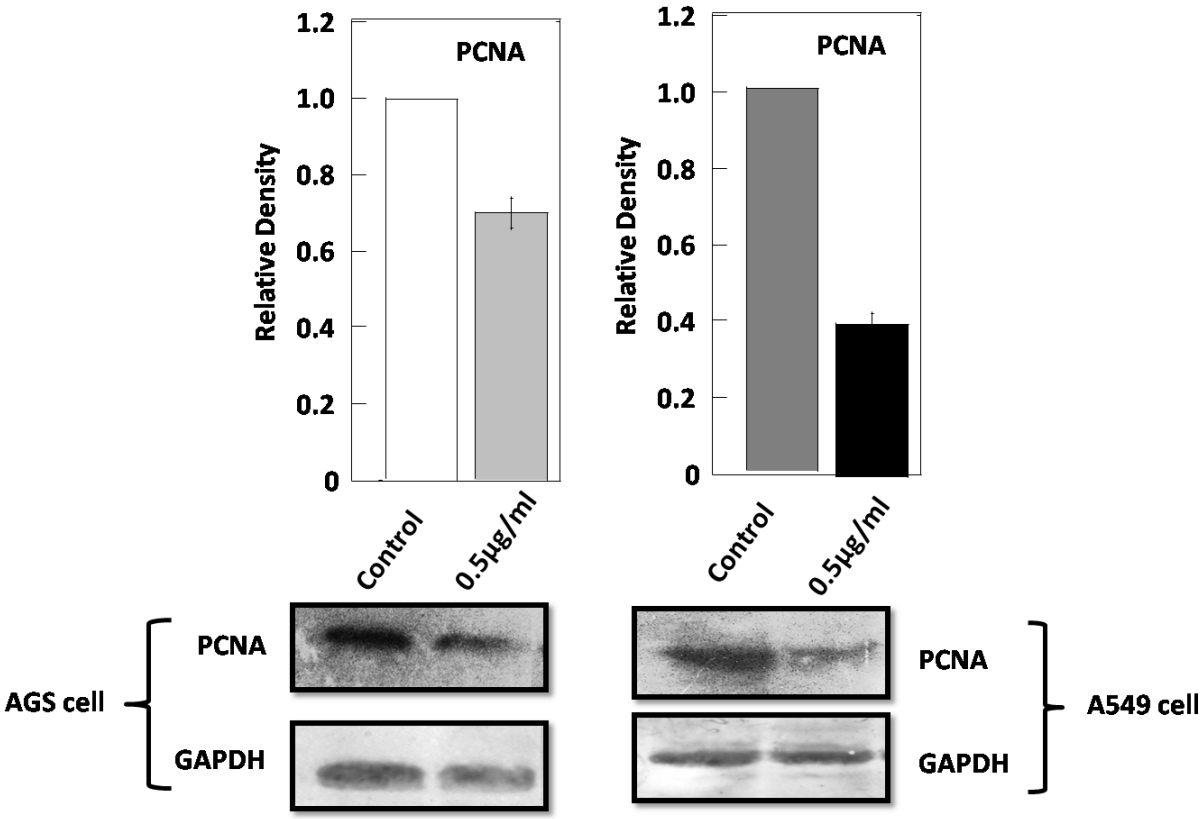
PCNA
Relative Density
1.2
1.0
0.8
0.6
0.4
0.2
0
Control
0.5μg/ml
AGS cell
PCNA
GAPDH
PCNA
Relative Density
1.2
1.0
0.8
0.6
0.4
0.2
0
Control
0.5μg/ml
PCNA
GAPDH
A549 cell

13A 13B

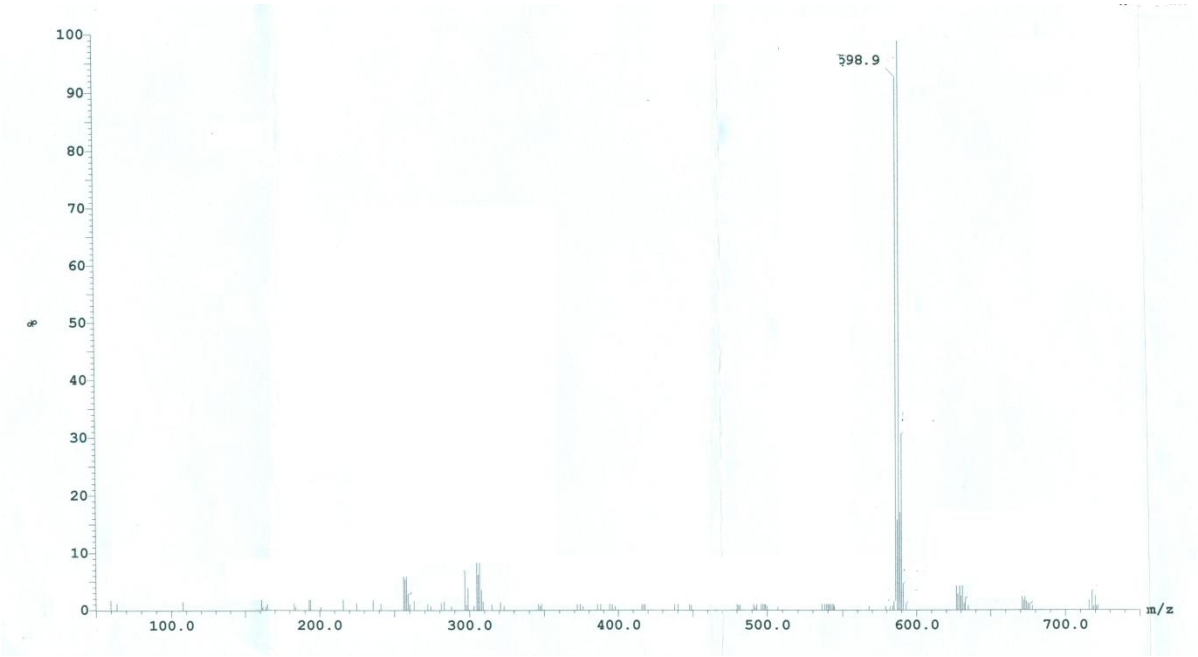

Fig. S 14 ESI-MS of complex **1**